

LETTER • OPEN ACCESS

## Diel, seasonal, and inter-annual variation in carbon dioxide effluxes from lakes and reservoirs

To cite this article: Malgorzata Golub *et al* 2023 *Environ. Res. Lett.* **18** 034046

View the [article online](#) for updates and enhancements.

You may also like

- [The pulsatility curve—the relationship between mean intracranial pressure and pulsation amplitude](#)  
Sara Qvarlander, Jan Malm and Anders Eklund
- [Validation of a novel method for continuous saline tonometry in a porcine model](#)  
R Frøjse, B Hedberg, T Bäcklund *et al.*
- [Resonance sensor measurements of stiffness variations in prostate tissue \*in vitro\*—a weighted tissue proportion model](#)  
Ville Jalkanen, Britt M Andersson, Anders Bergh *et al.*



### Breath Biopsy® OMNI®

The most advanced, complete solution for  
global breath biomarker analysis

TRANSFORM YOUR  
RESEARCH WORKFLOW



Expert Study Design  
& Management



Robust Breath  
Collection



Reliable Sample  
Processing & Analysis



In-depth Data  
Analysis



Specialist Data  
Interpretation

ENVIRONMENTAL RESEARCH  
LETTERS

## LETTER

## Diel, seasonal, and inter-annual variation in carbon dioxide effluxes from lakes and reservoirs

## OPEN ACCESS

## RECEIVED

28 September 2022

## REVISED

24 January 2023

## ACCEPTED FOR PUBLICATION

2 February 2023

## PUBLISHED

9 March 2023

Original content from this work may be used under the terms of the [Creative Commons Attribution 4.0 licence](#).

Any further distribution of this work must maintain attribution to the author(s) and the title of the work, journal citation and DOI.



Malgorzata Golub<sup>1</sup>, Nikaan Koupaei-Abyazani<sup>2</sup> , Timo Vesala<sup>3,4</sup>, Ivan Mammarella<sup>5</sup>, Anne Ojala<sup>6</sup>, Gil Bohrer<sup>7</sup>, Gesa A Weyhenmeyer<sup>8</sup>, Peter D Blanken<sup>9</sup>, Werner Eugster<sup>10,†</sup> , Franziska Koebsch<sup>11</sup>, Jiquan Chen<sup>12</sup> , Kevin Czajkowski<sup>13</sup>, Chandrashekhar Deshmukh<sup>14</sup>, Frederic Guérin<sup>15</sup>, Jouni Heiskanen<sup>16</sup>, Elyn Humphreys<sup>17</sup>, Anders Jonsson<sup>18</sup>, Jan Karlsson<sup>19</sup>, George Kling<sup>20</sup>, Xuhui Lee<sup>21</sup> , Heping Liu<sup>22</sup>, Annalea Lohila<sup>3,23</sup>, Erik Lundin<sup>24</sup> , Tim Morin<sup>25</sup>, Eva Podgrajsek<sup>26</sup>, Maria Provenzale<sup>27</sup>, Anna Rutgersson<sup>28</sup>, Torsten Sachs<sup>11</sup> , Erik Sahlée<sup>28</sup>, Dominique Serça<sup>29</sup> , Changliang Shao<sup>30</sup>, Christopher Spence<sup>31</sup>, Ian B Strachan<sup>32</sup> , Wei Xiao<sup>33</sup> and Ankur R Desai<sup>2,\*</sup>

<sup>1</sup> Dundalk Institute of Technology, Centre for Freshwater and Environmental Studies, Dundalk, Ireland

<sup>2</sup> Department of Atmospheric and Oceanic Sciences, University of Wisconsin-Madison, Madison, WI, United States of America

<sup>3</sup> Faculty of Science, University of Helsinki, Institute for Atmospheric and Earth System Research (INAR)/Physics, Helsinki, Finland

<sup>4</sup> Faculty of Agriculture and Forestry, University of Helsinki, INAR/Forest Sciences, Helsinki, Finland

<sup>5</sup> Faculty of Science, University of Helsinki, Institute for Atmospheric and Earth System Research (INAR)/Physics, Helsinki, Finland

<sup>6</sup> Natural Resources Institute Finland, Helsinki, Finland

<sup>7</sup> Department of Civil, Environmental and Geodetic Engineering, The Ohio State University, Columbus, OH, United States of America

<sup>8</sup> Department of Ecology and Genetics/Limnology, Uppsala University, Uppsala, Sweden

<sup>9</sup> Department of Geography, University of Colorado, Boulder, CO, United States of America

<sup>10</sup> ETH Zürich, Zürich, Switzerland

<sup>11</sup> GFZ German Research Centre for Geosciences, Potsdam, Germany

<sup>12</sup> Department of Geography, Environment and Spatial Science, Michigan State University, East Lansing, MI, United States of America

<sup>13</sup> Department of Geography and Planning, University of Toledo, Toledo, OH, United States of America

<sup>14</sup> APRIL Asia, Laboratoire d'Aérodynamique, Observatoire Midi-Pyrénées, Toulouse, France

<sup>15</sup> IRD—Marseille, Toulouse, France

<sup>16</sup> Faculty of Biological and Environmental Sciences, University of Helsinki, Helsinki, Finland

<sup>17</sup> Carleton University, Geography and Environmental Studies, Ottawa, Canada

<sup>18</sup> Umeå University, Department of Ecology and Environmental Science, Umeå, Sweden

<sup>19</sup> Department of Ecology and Environmental Science, Umeå University, Climate Impacts Research Centre (CIRC), Umeå, Sweden

<sup>20</sup> Department of Ecology and Evolutionary Biology, University of Michigan, Ann Arbor, MI, United States of America

<sup>21</sup> Yale University, School of the Environment, New Haven, CT, United States of America

<sup>22</sup> Department of Civil and Environmental Engineering, Washington State University, Pullman, WA, United States of America

<sup>23</sup> Finnish Meteorological Institute, Climate System Research, Helsinki, Finland

<sup>24</sup> Swedish Polar Research Secretariat, Abisko Scientific Research Station, Abisko, Sweden

<sup>25</sup> State University of New York, College of Environmental Science and Forestry, Syracuse, NY, United States of America

<sup>26</sup> OX2, Stockholm, Sweden

<sup>27</sup> University of Helsinki, Institute for Atmospheric and Earth System Research (INAR)/Department Physics, Helsinki, Finland

<sup>28</sup> Department of Earth Sciences, Uppsala University, Uppsala, Sweden

<sup>29</sup> Laboratoire d'Aérodynamique, Université de Toulouse, CNRS, UPS, Toulouse, France

<sup>30</sup> Institute of Agricultural Resources and Regional Planning, Chinese Academy of Agricultural Sciences, Beijing, People's Republic of China

<sup>31</sup> Environment and Climate Change Canada, Saskatoon, SK, Canada

<sup>32</sup> Department of Geography and Planning, Queen's University, Kingston, ON, Canada

<sup>33</sup> Nanjing University of Information Science and Technology, Yale-NUIST Center on Atmospheric Environment, Nanjing, Jiangsu, People's Republic of China

† Deceased.

\* Author to whom any correspondence should be addressed.

E-mail: [desai@aos.wisc.edu](mailto:desai@aos.wisc.edu)

**Keywords:** eddy covariance, freshwater systems, lakes, reservoirs, carbon flux, synthesis

Supplementary material for this article is available [online](#)

## Abstract

Accounting for temporal changes in carbon dioxide (CO<sub>2</sub>) effluxes from freshwaters remains a challenge for global and regional carbon budgets. Here, we synthesize 171 site-months of flux measurements of CO<sub>2</sub> based on the eddy covariance method from 13 lakes and reservoirs in the

Northern Hemisphere, and quantify dynamics at multiple temporal scales. We found pronounced sub-annual variability in CO<sub>2</sub> flux at all sites. By accounting for diel variation, only 11% of site-months were net daily sinks of CO<sub>2</sub>. Annual CO<sub>2</sub> emissions had an average of 25% (range 3%–58%) interannual variation. Similar to studies on streams, nighttime emissions regularly exceeded daytime emissions. Biophysical regulations of CO<sub>2</sub> flux variability were delineated through mutual information analysis. Sample analysis of CO<sub>2</sub> fluxes indicate the importance of continuous measurements. Better characterization of short- and long-term variability is necessary to understand and improve detection of temporal changes of CO<sub>2</sub> fluxes in response to natural and anthropogenic drivers. Our results indicate that existing global lake carbon budgets relying primarily on daytime measurements yield underestimates of net emissions.

## 1. Introduction

The global carbon budget is rapidly changing in response to anthropogenic emissions (Hanson *et al* 2006, Friedlingstein *et al* 2020). Prior studies have estimated that 0.14–0.64 Pg C–CO<sub>2</sub> is annually released to the atmosphere through lakes and reservoirs (Cole *et al* 1994, 2007, Aufdenkampe *et al* 2011, Ciais *et al* 2013, Raymond *et al* 2013, Holgersson and Raymond 2016, DelSontro *et al* 2018, Drake *et al* 2018). However, most of these estimates are made with relatively limited sampling, generally constrained to the open-water or summer season during the daytime, and with limited consideration of interannual and shorter-scale variation (Butman *et al* 2018, Ran *et al* 2021).

Underrepresentation of temporal changes and variability of carbon dioxide (CO<sub>2</sub>) flux in existing CO<sub>2</sub> flux inventories may bias estimates of lake CO<sub>2</sub> emissions (Deemer *et al* 2016, Klaus *et al* 2019). Recent studies have found nighttime emissions exceeding daytime emissions because of potential uptake in lakes (Shao *et al* 2015), reservoirs (Liu *et al* 2016), and rivers (Gómez-Gener *et al* 2021). A lack of frequent and long-term CO<sub>2</sub> observations also limits our ability to differentiate natural CO<sub>2</sub> flux variations from the consequences of anthropogenic perturbations (Hasler *et al* 2016). Multiyear-scale time series that capture sub-annual variability of the aquatic CO<sub>2</sub> flux remain rare (Huotari *et al* 2011, Shao *et al* 2015, Finlay *et al* 2019). Traditional *in-situ* aquatic sampling methods for CO<sub>2</sub> concentrations and fluxes in natural and artificial freshwaters also come with high uncertainty (Golub *et al* 2017, Baldocchi *et al* 2020), with one source being the heterogeneity of littoral and pelagic lake CO<sub>2</sub> fluxes (Erkkilä *et al* 2018, Spafford and Risk 2018).

Advances in the past several decades, however, have enabled more long-term, continuous high-frequency (hourly) measurements of CO<sub>2</sub> flux in freshwater ecosystems, which are capable of capturing the dynamics of air-water fluxes at time scales of hours to years (Eugster *et al* 2003, Huotari *et al* 2011, Morales-Pineda *et al* 2014, Shao *et al* 2015).

At these time scales, CO<sub>2</sub> fluxes have been shown to respond to variations in photosynthesis and respiration rates (Cole *et al* 2007), wind speed and direction (Podgrajsek *et al* 2015), carbonate equilibria (Atilla *et al* 2011), ecosystem metabolism (Provenza *et al* 2018), convective mixing (Eugster *et al* 2003, Mammarella *et al* 2015), internal waves (Heiskanen *et al* 2014), ice phenology (Reed *et al* 2018), chlorophyll a concentration (Shao *et al* 2015), atmospheric turbulence generated by surrounding topography (Eugster *et al* 2022), and hydrological and carbon inflows/outflows (Rantakari and Kortelainen 2005, Weyhenmeyer *et al* 2015). These sources of variation may be overlooked by low-frequency and season-restricted sampling that dominate freshwater science (Desai *et al* 2015).

A growing number of previous studies were conducted using eddy covariance (EC) flux towers, which measure ecosystem-scale air-water CO<sub>2</sub> fluxes (Vesala *et al* 2006) and has gained prominence for use in freshwaters (Vesala *et al* 2012). While its application over lakes has mostly covered short periods of time (e.g. Eugster *et al* 2003, Vesala *et al* 2006, Podgrajsek *et al* 2015), an increasing number of sites are now measuring lake-atmosphere fluxes continuously over multiple years (Huotari *et al* 2011, Mammarella *et al* 2015, Shao *et al* 2015, Franz *et al* 2016, Reed *et al* 2018, Eugster *et al* 2020). Other methods for high frequency sampling have also included the use of forced diffusion automated chambers (Spafford and Risk 2018, Rudberg *et al* 2021). Here, to identify modes of CO<sub>2</sub> flux variability missed by infrequent sampling from lakes and reservoirs, we quantify diel to inter-annual dynamics of CO<sub>2</sub> fluxes directly measured by EC towers in 13 lakes and reservoirs in the Northern Hemisphere, the first synthesis of this kind. Mutual information analysis is utilized to determine sources of temporal CO<sub>2</sub> flux variability at each site. Additionally, this dataset contains sites with a wide range of nutrient status (i.e. eutrophic, oligotrophic, and mesotrophic), therefore allowing for comparisons between temporal changes of CO<sub>2</sub> fluxes among different freshwater systems.

## 2. Materials and methods

### 2.1. Study sites

Data on air–water CO<sub>2</sub> exchange and meteorological drivers were acquired from 19 study sites across the Northern Hemisphere, with at least one season of observations between 2005–2015, of which 13 were retained here for analysis (tables 1 and S1). The six remaining submitted sites were withheld for challenges in meeting uncertainty and gap filling criteria (see supplemental methods). These sites were collected based on organization of a workshop (Desai *et al* 2015) and an open call through listservs. Selected sites included 9 lakes and 4 reservoirs, mostly located between 40°N and 68°N latitude, coinciding with the largest area of Earth covered with lakes. Eight sites had data available over multiple seasons, but only a few also had measurements during winter ice cover. Lake area ranged from 0.036 km<sup>2</sup> to 623 km<sup>2</sup> (median: 15.2 km<sup>2</sup>), with median mean depth of 6 m (range: 0.6–11 m); most developed a seasonal thermocline and were dimictic or monomictic (table S1). Two water bodies had a significant fraction of submerged and emergent macrophytes (SE-Tam and DE-Zrk) within the footprint of the flux tower.

### 2.2. Measurements

The EC technique directly measures the exchange of momentum, heat and matter (water vapor, CO<sub>2</sub>, or other trace gasses) at the air–water interface and is a reliable method for measuring surface exchanges with the atmosphere (Vesala *et al* 2006). The flux towers were located on floating platforms, lake shoals or islands, or on shore depending on the site (Supplemental Material Text; table S1). The towers were additionally equipped with instruments providing half-hourly to hourly measurements of biophysical variables (e.g. net radiation (*R*<sub>net</sub>), air temperature (*T*<sub>air</sub>) and humidity, photosynthetically-active radiation (PAR), 3D wind direction and speed, water surface temperature (*T*<sub>water</sub>), aquatic CO<sub>2</sub> or O<sub>2</sub> concentration, and water level), although data availability and frequency varied among the sites. Data were harmonized to uniform formats and units, screened for fetch, de-spiked, and gap-filled using a common flux post-processing standard prior to calculation of diel and monthly averages (Pastorello *et al* 2020; Supporting Material Text). Flux footprint and wind directional screening were applied by each investigator to retain only those half-hourly observations representative of the water body. Note that a negative CO<sub>2</sub> flux indicates uptake by the ecosystem from the atmosphere and a positive flux means the reverse. All data are published in the Environmental Data Initiative repository (Golub *et al* 2022).

### 2.3. Data analysis

We analyzed the half-hourly CO<sub>2</sub> fluxes and three major groups of biophysical covariates. The first

group included variables related to wind forcing acting on the water surface (i.e. friction velocity, wind speed, momentum flux). The second group encompassed variables related to temperature cycles and proxies of energy in the system (i.e. *T*<sub>air</sub>, *T*<sub>water</sub>,  $\Delta T$  (*T*<sub>water</sub> – *T*<sub>air</sub>), sensible (H) and latent heat (LE) fluxes). The last group included the variables associated with solar radiation—proxies for primary productivity (i.e.  $\Delta p\text{CO}_2$  (*p*CO<sub>2water</sub> – *p*CO<sub>2air</sub>), PAR). To determine the standardized difference between two means with repeated unpaired measurements and imbalanced population sizes, we used the Cohen's *d* test where the mean difference between the mean daily CO<sub>2</sub> fluxes is divided by the pooled variance. A coefficient *d* of 0.20, 0.50, 0.80 indicates small, medium, and large standardized differences between the two means, respectively.

To determine the degree of the net ecosystem exchange (NEE) predictability by biophysical drivers (i.e. *T*<sub>air</sub>, *T*<sub>water</sub>, H and LE, friction velocity (*U*<sub>star</sub>), and *R*<sub>net</sub>), we performed mutual information analysis (MI). MI measures the statistical dependence of a variable 'Y' on another variable 'X'. Using the marginal and joint probability distributions of 'X' and 'Y', it expresses the proportion of bits needed to represent 'Y' that is redundant given the knowledge of 'X'. There are also no parametric assumptions regarding the relationship between the two variables, making MI capable of discerning linear and non-linear associations (Knox *et al* 2021). More information on MI may be found in Fraser and Swinney (1986). Ultimately, this method can reveal dependencies between two variables with co-varying factors, making it a useful approach for ascertaining NEE dependencies on ecosystem variables (Knox *et al* 2021). We use mutual information scores (MIS) to determine the relative strength of each bivariate interaction. High and low MIS corresponds to a strong and weak link between NEE and biophysical variables, respectively.

To account for driver impacts on different temporal scales, we used the maximal-overlap discrete wavelet transform (MODWT) approach to decompose half-hourly data into four temporal scales (hourly, diel, multiday, and seasonal). MODWT involves applying a high-pass wavelet filter and low-pass scaling filter to the time series. This allows a decomposition of the time series into multiple fine and coarse scales, enabling analysis at varying timescales (Percival 1995, Percival and Walden 2000). We used the 'Wavelet Methods for Time Series Analysis' in MATLAB's 'Wavelet Toolkit' to decompose the data (Cornish *et al* 2003). Further details on the application of this method may be found in the supplement and Sturtevant *et al* (2016).

Finally, to quantify potential sample bias from infrequent sampling and identify optimal sampling approaches, a random sample analysis was conducted on the gap-filled oligotrophic (US-Too; 2012), mesotrophic (FI-Van; 2016), and eutrophic (DE-Zrk;

**Table 1.** Comparison of ice-free CO<sub>2</sub> flux at temporal (i.e. annual, seasonal, diurnal and nocturnal) scales derived from high-frequency eddy covariance measurements over lakes and reservoirs. CO<sub>2</sub> fluxes are presented as the mean ± one standard deviation. The numbers in brackets represent the number of observations integrated at a given time scale.

| Lake ID          | Name                                    | Year | Air-water CO <sub>2</sub> fluxes                        |   |  |  |
|------------------|---|------|---|---|--|--|
|                  |   |      | Annual totals<br>(gC m <sup>-2</sup> yr <sup>-1</sup> ) | Seasonal daily mean<br>(mgC m <sup>-2</sup> d <sup>-1</sup> ) | Daytime flux<br>(mgC m <sup>-2</sup> h <sup>-1</sup> ) | Nighttime flux<br>(mgC m <sup>-2</sup> h <sup>-1</sup> ) |
| CA-Dar<br>CA-Est | Daring Lake<br>Eastmain Reservoir       | 2006 | na  | 89 ± 157 (n = 95)   | 0.8 ± 10.7 (n = 1685)                                  | 12.2 ± 7.5 (n = 497)                                     |
|                  |   | 2008 | 119.1 (n = 214)   | 581 ± 398 (n = 214)   | 22.4 ± 27.5 (n = 2790)                                 | 26.2 ± 23.4 (n = 2117)                                   |
|                  |   | 2009 | 137.2 (n = 214)   | 610 ± 433 (n = 214)   | 21.9 ± 24.2 (n = 2786)                                 | 30.1 ± 25.1 (n = 2127)                                   |
|                  |   | 2010 | na  | 431 ± 335 (n = 214)   | 18 ± 20.8 (n = 2804)                                   | 17.9 ± 19.5 (n = 2108)                                   |
|                  |   | 2011 | 75.9 (n = 214)  | 367 ± 272 (n = 173)   | 15.2 ± 18.8 (n = 2399)                                 | 15.7 ± 15.7 (n = 1568)                                   |
|                  |   | 2012 | na (n = 214)  | na  | na   | na   |
| DE-Zrk           | Zarnekow Polder Reservoir               | 2013 | -126.1 (n = 214)  | 81 ± 880 (n = 170)  | -78.6 ± 111.6 (n = 2240)                               | 103.1 ± 47.5 (n = 1678)                                  |
|                  |   | 2014 | -190.7 (n = 214)  | -250 ± 835 (n = 214)  | -86 ± 104.1 (n = 2817)                                 | 81.4 ± 42 (n = 2098)                                     |
|                  |   | 2015 | -29.5 (n = 214)   | 396 ± 1148 (n = 214)  | -41.2 ± 101.2 (n = 2791)                               | 84.2 ± 54.6 (n = 2139)                                   |
|                  |   | 2010 | 31.4 (n = 214)  | 643 ± 140 (n = 58)  | 22.8 ± 13.9 (n = 670)                                  | 30.2 ± 13.8 (n = 656)                                    |
| FI-Kui           | Kuivajarvi Lake                         | 2011 | 107.9 (n = 214)   | 1047 ± 304 (n = 153)  | 39.7 ± 17.1 (n = 2075)                                 | 48.3 ± 21.2 (n = 1455)                                   |
|                  |   | 2012 | 91.5 (n = 241)  | 684 ± 274 (n = 169)   | 24.4 ± 16.5 (n = 1981)                                 | 32.4 ± 18.4 (n = 1893)                                   |
|                  |   | 2013 | 21.9 (n = 173)  | 304 ± 154 (n = 93)  | 8.8 ± 9.8 (n = 1201)                                   | 17.2 ± 9.9 (n = 939)                                     |
| FI-Pal<br>FI-VKa | Pallasjärvi Lake<br>Valkea-Kotinen Lake | 2003 | 59.7 (n = 209)  | 544 ± 155 (n = 208)   | 22 ± 7 (n = 2385)                                      | 23.4 ± 8.8 (n = 1848)                                    |
|                  |   | 2004 | 46.4 (n = 239)  | 450 ± 261 (n = 238)   | 16.5 ± 16.4 (n = 2986)                                 | 21 ± 13.6 (n = 2464)                                     |
|                  |   | 2005 | 31.1 (n = 227)  | 384 ± 215 (n = 226)   | 11.4 ± 15.3 (n = 2940)                                 | 22.6 ± 9.1 (n = 2103)                                    |
|                  |   | 2006 | 40.6 (n = 254)  | 472 ± 263 (n = 253)   | 15.8 ± 13 (n = 2983)                                   | 23.4 ± 13.4 (n = 2824)                                   |
|                  |   | 2007 | 43.6 (n = 222)  | 539 ± 232 (n = 221)   | 20.8 ± 11.3 (n = 3033)                                 | 24.5 ± 13.5 (n = 2038)                                   |
|                  |   | 2008 | -10.9 (n = 101)   | na  | na   | na   |
|                  |   | 2009 | na  | na  | na   | na   |

(Continued.)

Table 1. (Continued.)

|        |                        |      |                        |                             |                                |                                |
|--------|------------------------|------|------------------------|-----------------------------|--------------------------------|--------------------------------|
| FI-Van | Vänajavesi Lake        | 2016 | 105 ( <i>n</i> = 237)  | 457 ± 334 ( <i>n</i> = 237) | 17.6 ± 18.7 ( <i>n</i> = 2943) | 20.8 ± 17.8 ( <i>n</i> = 2505) |
| LA-NT2 | NamTheun 2 Reservoir   | 2017 | na                     | na                          | na                             | na                             |
|        |                        | 2008 | na                     | 1762 ± 186 ( <i>n</i> = 10) | 61 ± 17.8 ( <i>n</i> = 125)    | 87 ± 39.2 ( <i>n</i> = 106)    |
|        |                        | 2009 | na                     | 1623 ± 345 ( <i>n</i> = 15) | 73.5 ± 28.2 ( <i>n</i> = 146)  | 63.2 ± 29.7 ( <i>n</i> = 200)  |
|        |                        | 2010 | na                     | 861 ± 183 ( <i>n</i> = 4)   | 36 ± 16.3 ( <i>n</i> = 47)     | 35.3 ± 13.5 ( <i>n</i> = 46)   |
|        |                        | 2011 | na                     | na                          | na                             | na                             |
| SE-Mer | Merasjärvi Lake        | 2005 | 9 ( <i>n</i> = 165)    | 145 ± 149 ( <i>n</i> = 117) | 4.7 ± 9.4 ( <i>n</i> = 1877)   | 8.6 ± 9.3 ( <i>n</i> = 835)    |
| SE-Tam | Tamnaren Lake          | 2010 | 8.5 ( <i>n</i> = 216)  | 189 ± 125 ( <i>n</i> = 49)  | 6.9 ± 9.9 ( <i>n</i> = 493)    | 8.6 ± 11.4 ( <i>n</i> = 628)   |
|        |                        | 2011 | 28.5 ( <i>n</i> = 291) | 124 ± 161 ( <i>n</i> = 290) | 4.9 ± 11.2 ( <i>n</i> = 3619)  | 5.3 ± 10 ( <i>n</i> = 3027)    |
|        |                        | 2012 | na                     | 386 ± 176 ( <i>n</i> = 105) | 10.8 ± 12.3 ( <i>n</i> = 1663) | 27.4 ± 16.2 ( <i>n</i> = 743)  |
| US-UM3 | Douglas Lake           | 2013 | 46.8 ( <i>n</i> = 275) | 432 ± 318 ( <i>n</i> = 102) | 10.5 ± 25.9 ( <i>n</i> = 1374) | 28.5 ± 39 ( <i>n</i> = 965)    |
| US-RBa | Ross Barnett Reservoir | 2014 | 60.1 ( <i>n</i> = 275) | 412 ± 313 ( <i>n</i> = 142) | 9.6 ± 24.9 ( <i>n</i> = 1889)  | 27.7 ± 38.7 ( <i>n</i> = 1380) |
|        |                        | 2007 | 20.3 ( <i>n</i> = 365) | 162 ± 308 ( <i>n</i> = 129) | 5 ± 23.5 ( <i>n</i> = 1324)    | 8.4 ± 27.4 ( <i>n</i> = 1659)  |
| US-Too | Toolik Lake            | 2012 | na                     | 304 ± 130 ( <i>n</i> = 62)  | 8 ± 13 ( <i>n</i> = 1120)      | 28 ± 27.5 ( <i>n</i> = 308)    |



2014) lake/reservoir data with the smallest data gaps. One thousand random samples without replacement were taken for each of the following times: daytime-only (DT), daytime/nighttime-only (DT/NT), summer mid-day (SMD), growing season (GS), and annual. DT and NT were defined as 10:00–15:30 h and 22:00–03:30 h (local times), respectively. Hours between 11:00–13:30 h were considered mid-day while the GS counted fluxes between March 1st and September 30th. Flux counts of 1, 5, and 10 were taken at each temporal resolution to test dependencies of percent error (PE) on flux count within and between sites. To obtain a single flux value, the counts containing 5 and 10 fluxes were averaged. This sampling algorithm was created using Python version 3.8.3.

### 3. Results

#### 3.1. Magnitude of CO<sub>2</sub> fluxes

Study sites represented a wide range of nutrient-color status and physical characteristics of water bodies, and as a result spanned a range of daily CO<sub>2</sub> fluxes, although with some common elements (figure 1). The mean daily CO<sub>2</sub> flux across all sites was  $0.43 \pm 0.34 \mu\text{mol CO}_2 \text{ m}^{-2} \text{ s}^{-1}$  (mean  $\pm$  standard deviation, (SD); range:  $-0.075$ – $1.25 \mu\text{mol CO}_2 \text{ m}^{-2} \text{ s}^{-1}$ ) with only 6% of observations indicating neutral fluxes or net CO<sub>2</sub> uptake. The spread of time-resolved fluxes varied between 102% and 798% of the site-specific daily mean (figure 1). Reservoirs had smaller but more variable fluxes relative to the lakes ( $0.32 \pm 0.71$  vs.  $0.41 \pm 0.31 \mu\text{mol CO}_2 \text{ m}^{-2} \text{ s}^{-1}$ , respectively), although the reservoir sample size is smaller and more geographically restricted. Two thirds of sites had at least 66% of daily fluxes within the cross-site flux mean  $\pm 1$  SD (Cohen's  $d$ :  $0.02 < d < 0.76$ ).

Annually, all sites were CO<sub>2</sub> sources to the atmosphere, except for DE-Zrk and LA-NT2, with large variability across sites (figure 2). This was also the case when comparing the same lake or reservoir type. On a single day (on average), the mesotrophic and eutrophic lakes and reservoirs were the largest and smallest carbon sources, respectively. While most sites were a greater carbon source during the nighttime relative to the daytime, the difference in hourly fluxes was small ( $0.5 \mu\text{mol C m}^{-2} \text{ s}^{-1}$ ), except for DE-Zrk.

#### 3.2. Temporal variability

Averaged diel CO<sub>2</sub> changes had regular patterns of daytime minima and nighttime maxima across all sites in most months (figure 2(a)). Daytime hourly fluxes were on average 35% (range 7%–60%) lower than nighttime fluxes, though in 94% of site-days, those were still net positive emissions. Despite the commonly observed daytime CO<sub>2</sub> flux dip, the flux decrease was large enough to convert our sites to daily net sinks of CO<sub>2</sub> in only 11% of site-months. The

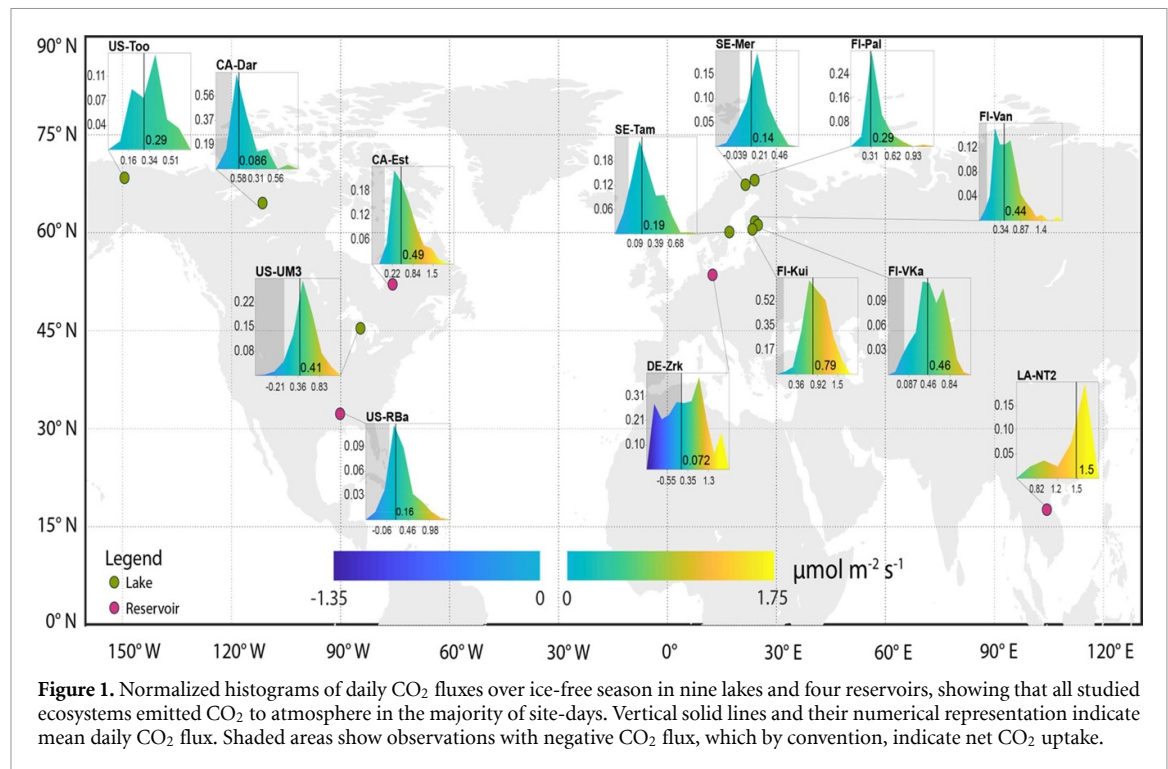
mean uncertainty of diel CO<sub>2</sub> was strongly influenced by extreme observations, with 192% mean uncertainty, but only 79% median uncertainty.

Maximum diel flux amplitudes occurred typically in July and August and ranged  $0.24$ – $1.09 \mu\text{mol CO}_2 \text{ m}^{-2} \text{ s}^{-1}$ . Relative to the summer amplitudes, shoulder season CO<sub>2</sub> flux amplitudes were on average 44%–49% smaller in May and September and 26%–37% in April and October. Monthly to sub-annual CO<sub>2</sub> flux variability was nearly twofold higher compared to the diel flux variation. Surprisingly, we found frequent sub-monthly (20–30 d) variability across all water bodies, regardless of the system's physical or biogeochemical conditions. While most site-level variability fluctuated around the CO<sub>2</sub> flux averages, for some, amplitudes scaled with flux minima and maxima (figure S1). Sites with multi-year data had relatively consistent sub-annual patterns across years, although the timing and amplitudes of sub-monthly variability varied among lake-years. When integrated over time-resolved daily CO<sub>2</sub> fluxes, both sub-monthly and sub-annual modes of variability accounted for two thirds of the site-level daily variability (range 10%–190%). Mean and median uncertainty were 167% and 67% of mean daily CO<sub>2</sub> flux, respectively.

Once scaled to ice-free season annual emissions, and assuming zero fluxes during ice cover, we found all water bodies were net sources of CO<sub>2</sub>, despite missing any ice off/on related fluxes (table 1). The cross-site mean and SD of 23 site-years was  $95 \pm 49 \text{ gC m}^{-2} \text{ yr}^{-1}$  (range:  $14$ – $224 \text{ gC m}^{-2} \text{ yr}^{-1}$ ). Inter-annual variability (IAV) was calculated as a SD of annual CO<sub>2</sub> flux for each site with multi-year data (figure S2). The mean cross-site IAV was  $22 \text{ gC m}^{-2} \text{ yr}^{-1}$  (25%) and ranged between 4 and  $44 \text{ gC m}^{-2} \text{ yr}^{-1}$  (3%–58%).

#### 3.3. Drivers of CO<sub>2</sub> fluxes

While the continuous data allowed capturing CO<sub>2</sub> flux variability at multiple temporal scales, we still had a limited capacity to attribute which factors and processes governed the CO<sub>2</sub> flux. We found small standardized differences between CO<sub>2</sub> fluxes among site groups belonging to the three humic states ( $d < 0.01$ ), medium differences between oligotrophic and eutrophic states ( $d = 0.24$ ), and large CO<sub>2</sub> differences between mesotrophic and oligotrophic states ( $d = 0.66$ ), and between mesotrophic and eutrophic states ( $d = 0.72$ ). Commonly observed biophysical covariates explained an average of 32% of variance in half-hourly CO<sub>2</sub> fluxes. Wind-related variables were identified as a key to explaining CO<sub>2</sub> flux variability in eight out of 13 sites. Biophysical variables related to exchanges of heat at the air-water interface, particularly  $\Delta T$  and turbulent energy exchange (H and LE), both correlated with CO<sub>2</sub> flux. The fitted regressions were non-linear and highly variable across sites, owing to ecosystem differences



and presence of confounding factors (e.g. differential responses to co-dependent covariates).

Mutual information analysis revealed different drivers to be responsible for CO<sub>2</sub> fluxes on different temporal scales (figure 4). On hourly scales, CO<sub>2</sub> flux at all sites was predicted mostly by  $T_{\text{air}}$  and  $T_{\text{water}}$ . The strongest links were found to occur at LA-NT2 and DE-Zrk, both being eutrophic systems. Analysis on diel scales yielded a similar result. On multi-day scales, however, more linkage between CO<sub>2</sub> flux and drivers was found at CA-Dar, SE-Mer, and FI-Pal (all oligotrophic). While the seasonal scale MI analysis was subject to many gaps, it did show a more uniform CO<sub>2</sub> flux prediction magnitude across all sites and drivers relative to other timescales.

### 3.4. Temporal analysis

Random sampling among different temporal resolutions resulted in large differences between mean sampled NEE and mean continuous annual NEE (figure S3). For DE-Zrk and FI-Van, the greatest PE was for samples taken during SMD, calculated to be  $868\% \pm 26\%$  and  $38\% \pm 2\%$  (mean  $\pm$  range), respectively. US-Too experienced the largest error during NT sampling, with a PE of  $87\% \pm 31\%$ . Increasing the number of NEE values per sample (i.e. going from 1 to 5 to 10 samples with the latter two NEE values calculated as the average) gave sporadic results, in that, agreement sometimes improved (FI-Van during GS) and sometimes worsened (US-Too during nighttime). DT/NT and annual sampling were the most representative of continuous annual NEE among all sites regardless of lake/reservoir type. GS sampling showed PE that was well within the typical

uncertainty for EC flux measurements ( $\sim 20\%$ ) for FI-Van and US-Too. Sampling on an annual scale further constrained PE, including even DE-Zrk in addition to FI-Van and US-Too.

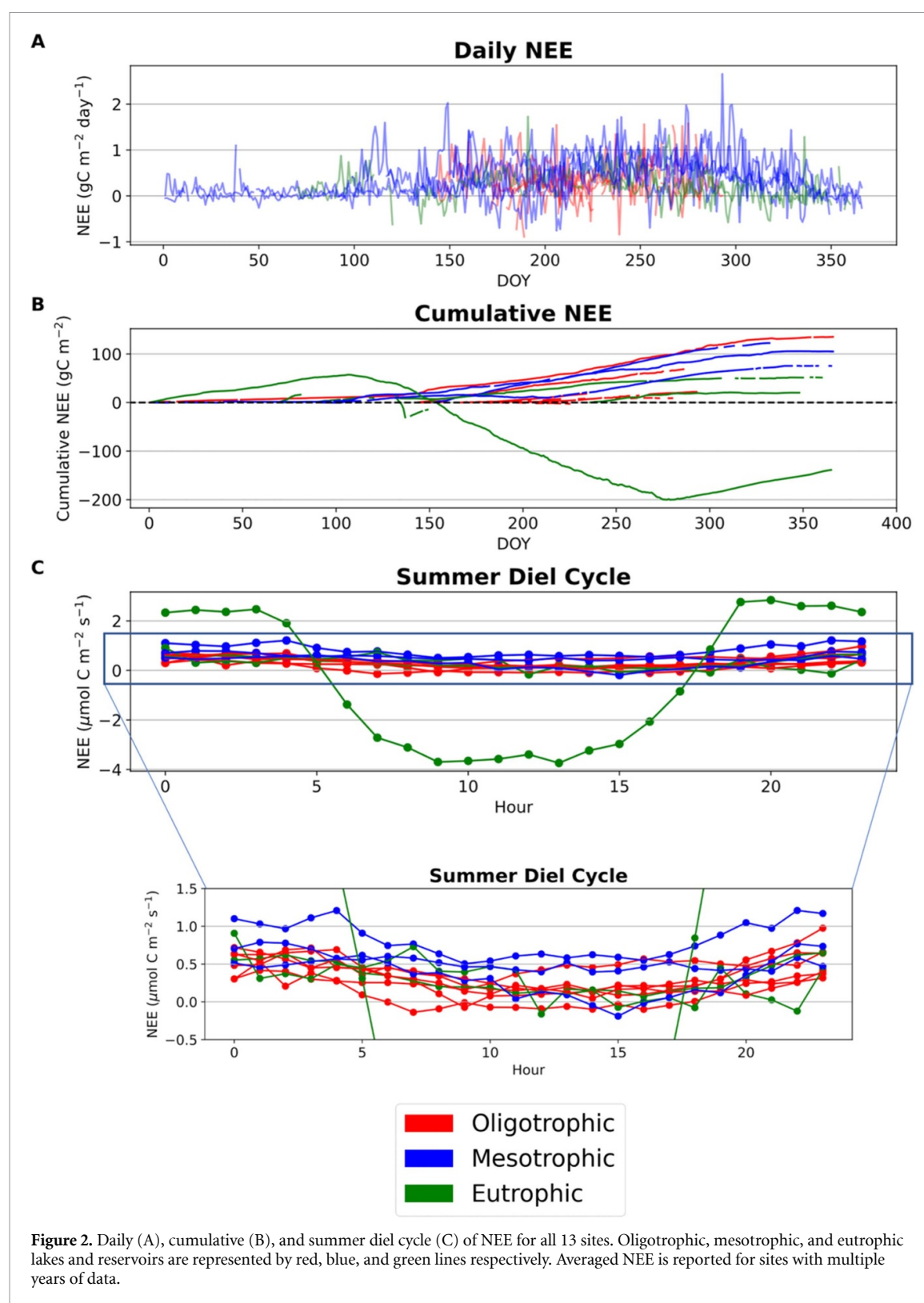
Bias was also calculated using the same random sampling method. This was defined as subtracting the mean continuous annual NEE from the mean sampled NEE at each site. Overall, DE-Zrk showed high bias across all temporal resolutions ( $-0.8 \pm 5.2 \mu\text{mol CO}_2 \text{ m}^{-2} \text{ s}^{-1}$ ) while US-Too and FI-Van had bias that was an order of magnitude smaller (figure 3).

## 4. Discussion

### 4.1. Forcing differences by type

Through this synthesis,  $T_{\text{water}}$  is shown to be a major predictor of lake and reservoir NEE, which is consistent with past work of Zwart *et al* (2019) and Eugster *et al* (2020). There is a high degree of spatiotemporal variability between these two variables. For example, NEE at LA-NT2 and DE-Zrk (eutrophic reservoir and eutrophic shallow lake respectively) was most highly predicted by  $T_{\text{water}}$  on short timescales (hourly and diel), suggesting these ecosystems may be most susceptible to evading CO<sub>2</sub> following climate warming. This large link may also be explicable through lake type. Eutrophic lakes are defined as being nutrient rich, meaning they contain larger phosphorus, nitrogen, or dissolved organic carbon concentrations (DOC) than their oligotrophic counterparts (Reed *et al* 2018). On multiday timescales, however, the distinguishability of the NEE/ $T_{\text{water}}$  linkage in the eutrophic sites is less prominent when

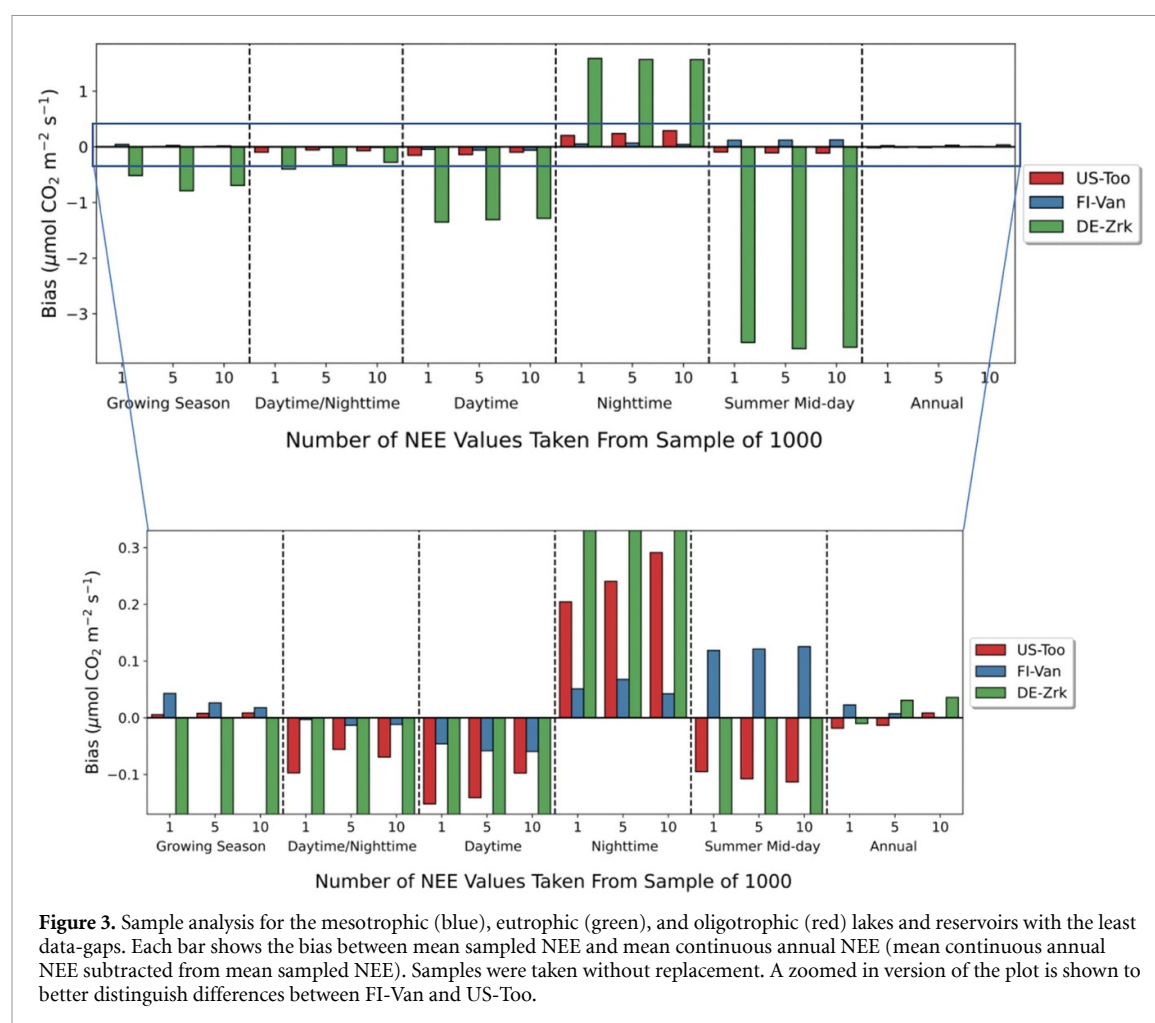




compared to the oligotrophic and mesotrophic sites. Another variable with high NEE predictability was  $T_{\text{air}}$ , though it is possible that in some cases fluxes have an indirect relationship with  $T_{\text{air}}$  via its impact on DOC input from land (Sobek *et al* 2005). Due to lack of significant findings, we excluded asynchronous driver analysis in this work. We acknowledge that these drivers are present in other studies

covering freshwater ecosystems such as in Sturtevant *et al* (2016).

Additionally, we acknowledge that there may have been  $\text{CO}_2$  flux variabilities due to lithological or geographical variables not discussed here. For example, López *et al* (2011) found  $\text{CO}_2$  dynamics to be weakly coupled to calcareous systems. León-Palmero *et al* (2020) noted reservoir  $\text{CO}_2$  fluxes to be dependent on



lithology, with a CO<sub>2</sub> source and sink being reported for calcareous and siliceous watersheds, respectively. The work also found an impact of reservoir mean depth on methane fluxes, which highlights that these influences are not limited to CO<sub>2</sub>. Water chemistry and carbon isotope data would also provide great insights on the contributions of dissolved inorganic carbon (DIC) transformation and organic carbon mineralization (Zhong *et al* 2018), especially in cases of damming where DIC transport is affected (Wang *et al* 2020). These processes have been documented to play an important role in CO<sub>2</sub> outgassing, but the limitations of our dataset prevented us from conducting further analysis on these processes. As a result, future studies must take these characteristics and processes into account due to their prominent role in influencing lake and reservoir greenhouse gas flux magnitudes across multiple temporal scales.

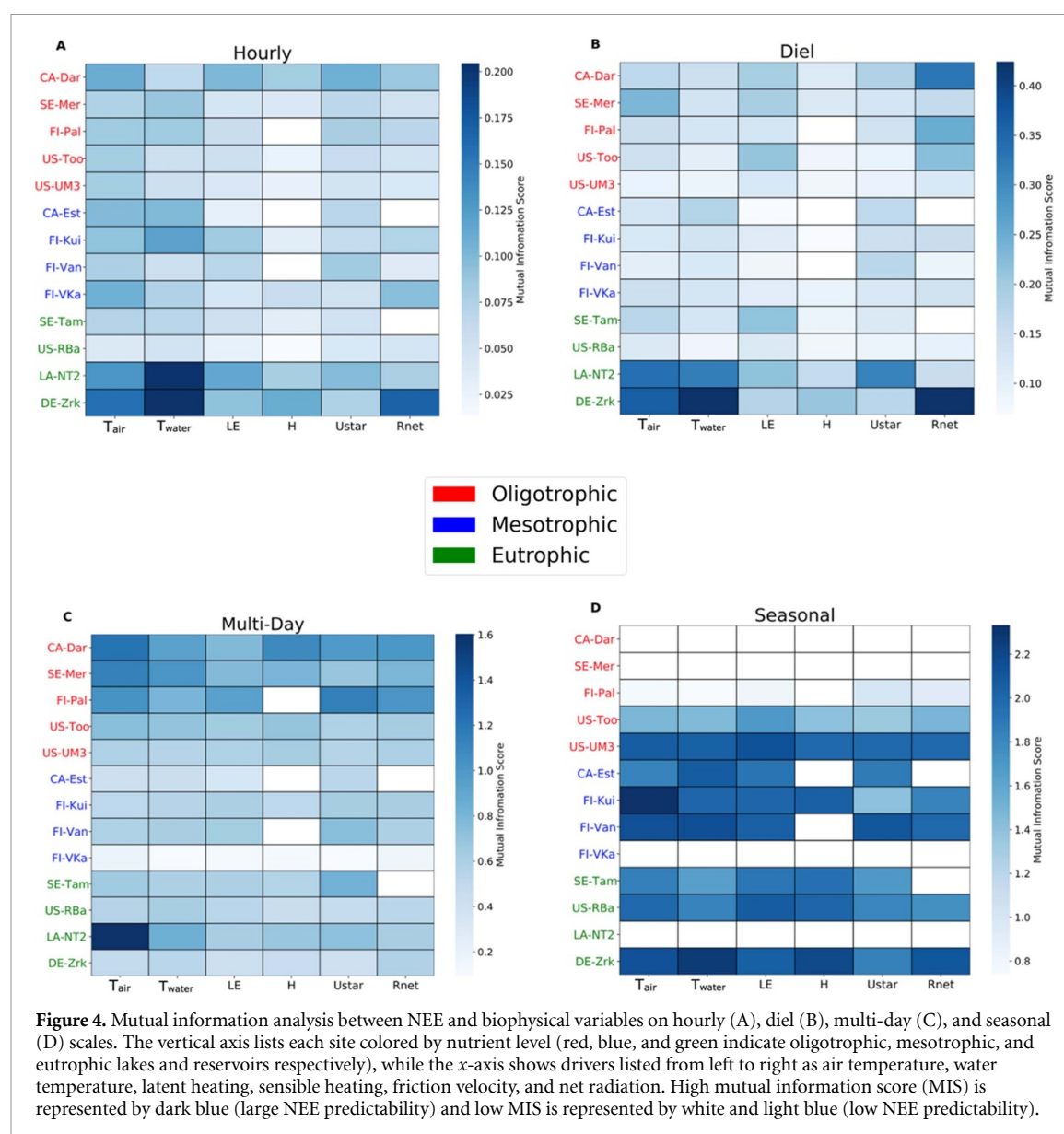
#### 4.2. Unresolved temporal variation in CO<sub>2</sub> fluxes

CO<sub>2</sub> fluxes from lakes and reservoirs exhibited large variability at diel to inter-annual scales, which could comprise unresolved sources of uncertainty or bias in current estimates of annual CO<sub>2</sub> fluxes from infrequent and season-restricted sampling. Although our study lakes were not randomly selected and cannot be

directly used to upscale (Stanley *et al* 2019), they were broadly reflective of common mid-latitude freshwater systems spanning a broad range of humic-status and mixing regimes. Additional considerations for measurements across lake size and catchment area (Hanson *et al* 2007, Holgersson and Raymond 2016) and hydrological setting (Jones *et al* 2018) would be required to design a representative estimate for global upscaling.

We were able to investigate, however, the role of temporal variation on a range of systems that broadly reflect many lakes and reservoirs. Our reported continuous daily fluxes corresponded to the upper end (88th percentile) of previously published flux magnitudes (table S2). The observed temporal variation suggests that temporal restrictions in sampling may add a significant source of underestimation bias in existing inventories of CO<sub>2</sub> fluxes from lakes and reservoirs of similar type and size (Klaus *et al* 2019).

In particular, we found large diel variation in all study sites, with routinely higher emissions at night, consistent with a recent study over rivers (Gómez-Gener *et al* 2021). Diel reduction of dissolved CO<sub>2</sub> concentrations and fluxes is often associated with ecosystem metabolism (Hanson *et al* 2003) and supported by negative correlations with



PAR, or even algal blooms (Shao *et al* 2015, Ouyang *et al* 2017). Water temperature (Provenza *et al* 2018), carbonate equilibria fluctuations (Atilla *et al* 2011), water-side convection (Eugster *et al* 2003, Mammarella *et al* 2015, Podgrajsek *et al* 2015), and internal waves (Heiskanen *et al* 2014) can additionally govern diel CO<sub>2</sub> dynamics. Our observed diel amplitudes were within 21%–43% of sub-hourly flux amplitudes derived from dissolved CO<sub>2</sub> concentrations (Hanson *et al* 2003, Morales-Pineda *et al* 2014) or previously published EC-measured fluxes (Vesala *et al* 2006, Liu *et al* 2016). Our results support the conclusion that existing global lake carbon budgets that rely primarily on daytime measurements are underestimates of net emissions.

We also found common sub-monthly modes of CO<sub>2</sub> flux variability across all of our sites. Similar variability in the continuous observations have been reported for dissolved CO<sub>2</sub> (Huotari *et al* 2009, Atilla *et al* 2011, Morales-Pineda *et al* 2014,

Vachon and Del Giorgio 2014) and CO<sub>2</sub> fluxes (Franz *et al* 2016, Eugster *et al* 2020), indicating the prevalence of oscillatory patterns in CO<sub>2</sub> time series at both sides of the air–water interface. Variability has been previously attributed to the interplay of wind forcing (Liu *et al* 2016), upwellings of CO<sub>2</sub>-rich waters (Morales-Pineda *et al* 2014), biologically-driven (metabolic and trophic) changes in carbonate equilibria (Atilla *et al* 2011, Ouyang *et al* 2017), convective mixing (Eugster *et al* 2003, Huotari *et al* 2009), non-local processes (Esters *et al* 2020), and  $T_{\text{water}}$  (Atilla *et al* 2011, Mammarella *et al* 2018). However, this is the first study to find a consistent pattern in a wide range of systems, regardless of size. We also observed changes to the prevalence of underlying sub-monthly CO<sub>2</sub> flux variability through the year at several sites, likely reflecting seasonal ecosystem changes, such as spring/fall turnover (Baehr and DeGrandpre 2004), radiative and heat exchanges (Heiskanen *et al* 2014), and hydrological inflows (Vachon *et al* 2017).

### 4.3. Implications for the global carbon budget

After our daily fluxes were scaled to site-specific annual CO<sub>2</sub> emission fluxes, estimates were in the upper end of previously reported estimates for lakes and reservoirs (table S2). All systems were sources of CO<sub>2</sub> in most years, although there have been sites that reported significant carbon sinks (e.g. Shao *et al* 2015, Reed *et al* 2018), and additional propagation of uncertainty from data gap filling and filtering (e.g. of nighttime uptake) can weakly push some of our study sites toward sinks. While our lakes are not fully representative of all lakes on Earth, we postulate that improved temporal resolution of site-level CO<sub>2</sub> fluxes is one of the sources of differences between this study and published annual fluxes (table S2). The results also imply that a proposed recommended number of samples per year (4–8) (Natchimuthu *et al* 2017, Klaus *et al* 2019) is likely insufficient to constrain annual CO<sub>2</sub> fluxes from lakes and reservoirs. Rather, our sampling analysis suggests to increase nighttime and open-water season observations, preferably weekly, which would reliably increase the accuracy of annual estimates, given our observed diel and sub-monthly variations.

Additionally, sites with multiple years of data all showed non-trivial interannual variation. The estimate of average IAV of CO<sub>2</sub> fluxes (25%) is modest compared to that (88%) observed in terrestrial ecosystems (Baldocchi *et al* 2018), partially reflecting the lower number and diversity of ecosystems with multi-year measurements or more buffering against climate extremes by large water bodies. However, given that CO<sub>2</sub> flux from freshwaters positively scales with the productivity of terrestrial ecosystems at shorter timescales (Walter *et al* 2021, Butman *et al* 2016, Hastie *et al* 2018), it is possible that the interannual variation of carbon input from land will propagate onto CO<sub>2</sub> evaded through freshwaters (McDonald *et al* 2013, Drake *et al* 2018), providing a possible pathway to better characterize freshwater IAV. Neglecting this variation is an additional source of bias in our current view on global CO<sub>2</sub> emissions from lakes and reservoirs.

Given that the CO<sub>2</sub> fluxes are affected at both sides of the air–water interface (Wanninkhof *et al* 2009), a better measure of the contribution of lakes to the global carbon cycle will also require reporting and synthesis of additional continuous water-side data (e.g. temperature, dissolved CO<sub>2</sub> and O<sub>2</sub>), site-level ecosystem characteristics (e.g. nutrient-color legacies, ecosystem metabolism, and aquatic vegetation such as algae), surrounding topography (Eugster *et al* 2022), and sampling an increased site diversity within climatic zones (Lehner and Döll 2004). With more frequent air and aquatic observations, we will better constrain CO<sub>2</sub> fluxes at different time scales, assess the prevalence of temporal patterns in CO<sub>2</sub> fluxes, and reduce uncertainty in eddy flux measurements over freshwaters

(e.g. Ejarque *et al* 2021) and therefore improve model estimates of responses of these ecosystems to climate change. These estimates will also allow for a robust representation of different climate variable effects on these fluxes (Sobek *et al* 2005). Such work will be needed to quantify and evaluate landscape (Buffam *et al* 2011, Zwart *et al* 2018) to global (DelSontro *et al* 2018) carbon budget components from lakes and reservoirs.

## 5. Conclusions

Across the 13 study sites with EC flux observations, all lakes and reservoirs were, on average, net annual sources of CO<sub>2</sub> to the atmosphere. However, the time series revealed large diel to (sub)-monthly CO<sub>2</sub> flux variability among the sites that represent a broad range of biogeochemical and physical site characteristics. These modes of variability accounted for two thirds of daily and a quarter of annual CO<sub>2</sub> flux variation, with sub-annual variability dominating over diel and inter-annual flux variabilities. After integrating these modes of variability into time-resolved fluxes, the CO<sub>2</sub> flux estimates were at the upper end of published CO<sub>2</sub> emissions for lakes and reservoirs. Our results support the idea that long-term, frequent measurements during both day and night of carbon dynamics in freshwater aquatic systems are critical to resolve lake NEE magnitudes and detect long-term trends of lake carbon fluxes. Omitting these temporal scales will not only limit our knowledge of lake NEE, but also restrict our understanding of biophysical driver impacts. We advocate for establishing and maintaining a long-term observation network that combines EC flux measurements with highly detailed site-specific carbon budget studies over key lake and reservoir ecosystems representing broader geographical gradients.

## Data availability statement

The data that support the findings of this study are openly available at the following URL/DOI: [10.6073/pasta/87a35ca843d8739d75882520c724e99e](https://doi.org/10.6073/pasta/87a35ca843d8739d75882520c724e99e).

## Acknowledgments

We thank all project participants for kindly sharing data and time. All flux tower data and code for processing data will be publicly available in the Environmental Data Initiative depository (DOI pending). MG and ARD acknowledge support from the U.S. National Science Foundation North Temperate Lakes LTER (NSF DEB-1440297, NTL LTER). Funding for US-UM3 was provided by the U.S. Department of Energy's Office of Science. IM and TV thank the support by the EU-Horizon Europe project 101056921—GreenFeedBack and Academy Professor projects (312571 and 282842). IM, TV and AL thank



the support from the ACCC Flagship funded by the Academy of Finland (337549 and 337552) and ICOS-Finland by University of Helsinki and the Ministry of Transport and Communication. GAW was financially supported by the Swedish Research Council (VR: Grant Nos. 2016-04153 and 2020-03222). The deployment of the EC at the Nam Theun 2 Reservoir (Lao PDR) was funded by Electricité de France (EDF) and Nam Theun Power Company (NTPC). TS and FK were supported by the Helmholtz Association of German Research Centres through grants to TS (Grant VH-NG-821) and FK (Grant PD-129), the Helmholtz Climate Initiative REKLIM (Regional Climate Change), and infrastructure funding through the Terrestrial Environmental Observatories Network (TER-ENO). TS and FK thank the (staff of the) Department Chemical Analytics and Biogeochemistry at the Leibniz-Institute of Freshwater Ecology and Inland Fisheries (Berlin) for providing water chemistry data for DE-Zrk. WE and GK acknowledge support from NSF-DEB 1637459 and OPP 1936769. The deployment of the flux tower at CA-Eastmain was supported by Hydro Quebec. Flux observations at US-OWC were funded by the Ohio Department of Natural Resources, by NOAA's National Estuarine Research Reserves' Davidson Fellowship, and by US Department of Energy awards DE-SC0021067 and DE-SC0022191. The co-authors express gratitude for the kindness and contributions of posthumous co-author Werner Eugster.

## Open research

We have deposited all EC lake observations and gap-filled values in the Environmental Data Initiative repository Golub *et al* (2022). Several sites are also accessible from FLUXNET affiliated archives as noted in table S2.



## Author contribution statement

M G designed experimental protocol and conducted the data syntheses. N K -A. conducted additional analyses and revisions. A R D, N K -A., and M G wrote the manuscript. T V, I M, G B, and G W supervised research, contributed observations, and edited the manuscript. All other authors contributed with flux observations and commented on the manuscript.

## Conflict of interest


The authors declare no competing financial interests

## ORCID iDs

Nikaan Koupaei-Abyazani  <https://orcid.org/0000-0001-6982-230X>  
Werner Eugster  <https://orcid.org/0000-0001-6067-0741>

Jiquan Chen  <https://orcid.org/0000-0003-0761-9458>

Xuhui Lee  <https://orcid.org/0000-0003-1350-4446>

Erik Lundin  <https://orcid.org/0000-0002-3785-8305>

Torsten Sachs  <https://orcid.org/0000-0002-9959-4771>

Dominique Serça  <https://orcid.org/0000-0001-8688-1440>

Ian B Strachan  <https://orcid.org/0000-0001-6457-5530>

## References

- Atilla N, McKinley G, Bennington V, Baehr M, Urban N, DeGrandpre M, Desai A R and Wu C 2011 Observed variability of Lake Superior pCO<sub>2</sub> *Limnol. Oceanogr.* **53** 775–86
- Aufdenkampe A K, Mayorga E, Raymond P A, Melack J M, Doney S C, Alin S R, Aalto R E and Yoo K 2011 Riverine coupling of biogeochemical cycles between land, oceans, and atmosphere *Front. Ecol. Environ.* **9** 53–60
- Baehr M M and DeGrandpre M D 2004 *In situ* pCO<sub>2</sub> and O<sub>2</sub> measurements in a lake during turnover and stratification: observations and modeling *Limnol. Oceanogr.* **49** 330–40
- Baldocchi A, Reed D E, Loken L, Stanley E, Huerd H and Desai A R 2020 Resolving space and time variation of lake-atmosphere carbon dioxide fluxes using multiple methods *J. Geophys. Res.* **125** e2019JG005623
- Baldocchi D, Chu H and Reichstein M 2018 Inter-annual variability of net and gross ecosystem carbon fluxes: a review *Agric. For. Meteorol.* **249** 520–33
- Buffam I, Turner M G, Desai A R, Hanson P C, Rusak J A, Lottig N R, Stanley E H and Carpenter S R 2011 Integrating aquatic and terrestrial components to construct a complete carbon budget for a north temperate lake district *Glob. Change Biol.* **17** 1193–211
- Butman D *et al* 2018 Inland waters *Second State of the Carbon Cycle Report (SOCCR2): A Sustained Assessment Report* ed N Cavallaro *et al* (Washington, DC: U.S. Global Change Research Program) pp 568–95
- Butman D, Stackpole S, Stets E, McDonald C P, Clow D W and Striegl R G 2016 Aquatic carbon cycling in the conterminous United States and implications for terrestrial carbon accounting *Proc. Natl Acad. Sci.* **113** 58–63
- Ciais P *et al* 2013 Carbon and other biogeochemical cycles *Climate Change 2013: The Physical Science Basis. Contribution of Working Group I to the Fifth Assessment Report of the Intergovernmental Panel on Climate Change* ed T F Stocker *et al* (Cambridge: Cambridge University Press) pp 465–570
- Cole J J *et al* 2007 Plumbing the global carbon cycle: integrating inland waters into the terrestrial carbon budget *Ecosystems* **10** 172–85
- Cole J J, Caraco N F, Kling G W and Kratz T K 1994 Carbon dioxide supersaturation in the surface waters of lakes *Science* **265** 1568–70
- Cornish C R, Percival D B and Bretherton C S 2003 The WMTSA Wavelet Toolkit for data analysis in the geosciences *EOS Trans. Am. Geophys. Union* **84** NG11A–0173
- Deemer B R, Harrison J A, Li S, Beaulieu J J, DelSontro T, Barros N, Bezerra-Neto J F, Powers S M, Dos santos M A and Vonk J A 2016 Greenhouse gas emissions from reservoir water surfaces: a new global synthesis *BioScience* **66** 949–64
- DelSontro T, Beaulieu J J and Downing J A 2018 Greenhouse gas emissions from lakes and impoundments: upscaling in the face of global change *Limnol. Oceanogr.* **3** 64–75
- Desai A R, Vesala T and Rantakari M 2015 Measurements, modeling, and scaling of inland water gas exchange *EOS* **96**
- Drake T W, Raymond P A and Spencer R G M 2018 Terrestrial carbon inputs to inland waters: a current



- synthesis of estimates and uncertainty *Limnol. Oceanogr.* **3** 132–42
- Ejarque E, Scholz K, Wohlfahrt G, Battin T J, Kainz M J and Schelker J 2021 Hydrology controls the carbon mass balance of a mountain lake in the eastern European Alps *Limnol. Oceanogr.* **66** 2110–25
- Erkkilä K-M, Ojala A, Bastviken D, Biermann T, Heiskanen J J, Lindroth A, Peltola O, Rantakari M, Vesala T and Mammarella I 2018 Methane and carbon dioxide fluxes over a lake: comparison between eddy covariance, floating chambers and boundary layer method *Biogeosciences* **15** 429–45
- Esters L, Rutgersson A, Nilsson E and Sahlee E 2020 Non-local impacts on eddy-covariance air-lake CO<sub>2</sub> fluxes *Bound.-Layer Meteorol.* **178** 283–300
- Eugster W *et al* 2003 CO<sub>2</sub> exchange between air and water in an arctic Alaskan and midlatitude Swiss lake: importance of convective mixing *J. Geophys. Res.* **108** 4362
- Eugster W, DelSontro T, Laundre J A, Dobkowski J, Shaver G R and Kling G W 2022 Effects of long-term climate trends on the methane and CO<sub>2</sub> exchange processes of Toolik Lake, Alaska *Front. Environ. Sci.* **10** 1–22
- Eugster W, DelSontro T, Shaver G R and Kling G W 2020 Interannual, summer, and diel variability of CH<sub>4</sub> and CO<sub>2</sub> effluxes from Toolik Lake, Alaska, during the ice-free periods 2010–2015 *Environ. Sci.: Process. Impacts* **22** 2181–98
- Finlay K, Vogt R J, Simpson G L and Leavitt P R 2019 Seasonality of pCO<sub>2</sub> in a hard-water lake of the northern Great Plains: the legacy effects of climate and limnological conditions over 36 years *Limnol. Oceanogr.* **64** S118–29
- Franz D, Koebsch F, Larmanou E, Augustin J and Sachs T 2016 High net CO<sub>2</sub> and CH<sub>4</sub> release at a eutrophic shallow lake on a formerly drained fen *Biogeosciences* **13** 3051–70
- Fraser A M and Swinney H L 1986 Independent coordinates for strange attractors from mutual information *Phys. Rev. A* **33** 1134–40
- Friedlingstein P *et al* 2020 Global carbon budget 2020 *Earth Syst. Sci. Data* **12** 3269–340
- Golub M *et al* 2022 Half-hourly gap-filled northern hemisphere lake and reservoir carbon flux and micrometeorology, 2006–2015 ver 1 (Environmental Data Initiative) (<https://doi.org/10.6073/pasta/87a35ca843d8739d75882520c724e99e>)
- Golub M, Desai A R, McKinley G A, Remucal C K and Stanley E H 2017 Large uncertainty in estimating pCO<sub>2</sub> from carbonate equilibria in lakes *J. Geophys. Res.* **122** 2909–24
- Gómez-Gener L *et al* 2021 Global carbon dioxide efflux from rivers enhanced by high nocturnal emissions *Nat. Geosci.* **14** 289–94
- Hanson P C, Bade D L, Carpenter S R and Kratz T K 2003 Lake metabolism: relationships with dissolved organic carbon and phosphorus *Limnol. Oceanogr.* **48** 1112–9
- Hanson P C, Carpenter S R, Armstrong D E, Stanley E H and Kratz T K 2006 Lake dissolved inorganic carbon and dissolved oxygen: changing drivers from days to decades *Ecol. Monogr.* **76** 343–63
- Hanson P C, Carpenter S R, Cardille J A, Coe M T and Winslow L A 2007 Small lakes dominate a random sample of regional lake characteristics *Freshw. Biol.* **52** 814–22
- Hasler C T, Butman D, Jeffrey J D and Suski C D 2016 Freshwater biota and rising pCO<sub>2</sub>? *Ecol. Lett.* **19** 98–108
- Hastie A, Lauerwald R, Weyhenmeyer G, Sobek S, Verpoorter C and Regnier P 2018 CO<sub>2</sub> evasion from boreal lakes: revised estimate, drivers of spatial variability, and future projections *Glob. Change Biol.* **24** 711–28
- Heiskanen J J, Mammarella I, Haapanala S, Pumpanen J, Vesala T, Macintyre S and Ojala A 2014 Effects of cooling and internal wave motions on gas transfer coefficients in a boreal lake *Tellus B* **66** 22827
- Holgersson M A and Raymond P A 2016 Large contribution to inland water CO<sub>2</sub> and CH<sub>4</sub> emissions from very small ponds *Nat. Geosci.* **9** 222–6
- Huotari J *et al* 2009 Temporal variations in surface water CO<sub>2</sub> concentration in a boreal humic lake based on high-frequency measurements *Boreal Environ. Res.* **14** 48–60
- Huotari J, Ojala A, Peltomaa E, Nordbo A, Launiainen S, Pumpanen J, Rasilo T, Hari P and Vesala T 2011 Long-term direct CO<sub>2</sub> flux measurements over a boreal lake: five years of eddy covariance data *Geophys. Res. Lett.* **38** L18401
- Jones S E, Zwart J A, Kelly P T and Solomon C T 2018 Hydrologic setting constrains lake heterotrophy and terrestrial carbon fate *Limnol. Oceanogr.* **3** 256–64
- Klaus M, Seekell D A, Lidberg W and Karlsson J 2019 Evaluations of climate and land management effects on lake carbon cycling need to account for temporal variability in CO<sub>2</sub> concentrations *Glob. Biogeochem. Cycles* **33** 243–65
- Knox S H *et al* 2021 Identifying dominant environmental predictors of freshwater wetland methane fluxes across diurnal to seasonal time scales *Glob. Change Biol.* **27** 3582–604
- Lehner B and Döll P 2004 Development and validation of a global database of lakes, reservoirs and wetlands *J. Hydrol.* **296** 1–22
- León-Palmero E, Morales-Baquero R and Reche I 2020 Greenhouse gas fluxes from reservoirs determined by watershed lithology, morphometry, and anthropogenic pressure *Environ. Res. Lett.* **15** 044012
- Liu H, Zhang Q, Katul G G, Cole J J, Chapin F S and MacIntyre S 2016 Large CO<sub>2</sub> effluxes at night and during synoptic weather events significantly contribute to CO<sub>2</sub> emissions from a reservoir *Environ. Res. Lett.* **11** 064001
- López P, Marcé R and Armengol J 2011 Net heterotrophy and CO<sub>2</sub> evasion from a productive calcareous reservoir: adding complexity to the metabolism-CO<sub>2</sub> evasion issue, *J. Geophys. Res.* **116** G02021
- Mammarella I *et al* 2015 Carbon dioxide and energy fluxes over a small boreal lake in Southern Finland: CO<sub>2</sub> and energy fluxes over lake *J. Geophys. Res.* **120** 1296–314
- Mammarella I *et al* 2018 Effects of similar weather patterns on the thermal stratification, mixing regimes and hypolimnetic oxygen depletion in two boreal lakes with different water transparency *Boreal Environ. Res.* **23** 237–47
- McDonald C P, Stets E G, Striegl R G and Butman D 2013 Inorganic carbon loading as a primary driver of dissolved carbon dioxide concentrations in the lakes and reservoirs of the contiguous United State *Glob. Biogeochem. Cycles* **27** 285–95
- Morales-Pineda M, Cózar A, Laiz I, Úbeda B and Gálvez J Á 2014 Daily, biweekly, and seasonal temporal scales of pCO<sub>2</sub> variability in two stratified Mediterranean reservoirs *J. Geophys. Res.* **119** 509–20
- Natchimuthu S, Sundgren I, Gålfalk M, Klemedtsson L and Bastviken D 2017 Spatiotemporal variability of lake pCO<sub>2</sub> and CO<sub>2</sub> fluxes in a hemiboreal catchment *J. Geophys. Res.* **122** 30–49
- Ouyang Z, Shao C, Chu H, Becker R, Bridgeman T, Stepien C, John R and Chen J 2017 The effect of algal blooms on carbon emissions in western lake Erie: an integration of remote sensing and eddy covariance measurements *Remote Sens.* **9** 44
- Pastorello G, Trotta C and Canfora E 2020 The FLUXNET2015 dataset and the ONEFlux processing pipeline for eddy covariance data *Sci. Data* **7** 225
- Percival D B and Walden A T 2000 *Wavelet Methods for Time Series Analysis* (Cambridge: Cambridge University Press)
- Percival D P 1995 On estimation of the wavelet variance *Biometrika* **82** 619–31
- Podgrajsek E, Sahlée E and Rutgersson A 2015 Diel cycle of lake-air CO<sub>2</sub> flux from a shallow lake and the impact of waterside convection on the transfer velocity *J. Geophys. Res.* **120** 29–38
- Provenzale M, Ojala A, Heiskanen J, Erkkilä K-M, Mammarella I, Hari P and Vesala T 2018 High-frequency productivity estimates for a lake from free-water CO<sub>2</sub> concentration measurements *Biogeosciences* **15** 2021–32

- Ran L, Butman D E, Battin T J, Yang X, Tian M, Duvert C, Hartmann J, Geeraert N and Liu S 2021 Substantial decrease in CO<sub>2</sub> emissions from Chinese inland waters due to global change *Nat. Commun.* **12** 1730
- Rantakari M and Kortelainen P 2005 Interannual variation and climatic regulation of the CO<sub>2</sub> emission from large boreal lakes *Glob. Change Biol.* **11** 1368–80
- Raymond P A et al 2013 Global carbon dioxide emissions from inland waters *Nature* **503** 355–9
- Reed D R, Dugan H, Flannery A and Desai A R 2018 Carbon sink and source dynamics of a eutrophic deep lake using multiple flux observations over multiple years *Limnol. Oceanogr.* **3** 285–92
- Rudberg D et al 2021 Diel variability of CO<sub>2</sub> emissions from northern lakes *J. Geophys. Res.* **126** e2021JG006246
- Shao C, Chen J, Stepien C A, Chu H, Ouyang Z, Bridgeman T B, Czajkowski K P, Becker R H and John R 2015 Diurnal to annual changes in latent, sensible heat, and CO<sub>2</sub> fluxes over a Laurentian Great Lake: a case study in Western Lake Erie *J. Geophys. Res.* **120** 1587–604
- Sobek S et al 2005 Temperature independence of carbon dioxide supersaturation in global lakes *Glob. Biogeochem. Cycles* **19**
- Spafford L and Risk D 2018 Spatiotemporal variability in lake-atmosphere net CO<sub>2</sub> exchange in the littoral zone of an oligotrophic lake *J. Geophys. Res.* **123** 1260–76
- Stanley E H, Collins S M, Lottig N R, Oliver S K, Webster K E, Cheruvilil K S and Soranno P A 2019 Biases in lake water quality sampling and implications for macroscale research *Limnol. Oceanogr.* **64** 1572–85
- Sturtevant C, Ruddell B, Knox S, Verfaillie J, Matthes J, Oikawa P and Baldocchi D 2016 Identifying scale-emergent, nonlinear, asynchronous processes of wetland methane exchange *J. Geophys. Res.* **121** 188–204
- Vachon D and Del Giorgio P A 2014 Whole-lake CO<sub>2</sub> dynamics in response to storm events in two morphologically different lakes *Ecosystems* **17** 1338–53
- Vachon D, Solomon C T and Del Giorgio P A 2017 Reconstructing the seasonal dynamics and relative contribution of the major processes sustaining CO<sub>2</sub> emissions in northern lakes: lake CO<sub>2</sub> seasonal dynamics *Limnol. Oceanogr.* **62** 706–22
- Vesala T, Eugster W and Ojala A 2012 Eddy covariance measurements over lakes *Eddy Covariance: A Practical Guide to Measurement and Data Analysis* ed M Aubinet, T Vesala and D Papale (Dordrecht: Springer) pp 365–76
- Vesala T, Huotari J, Rannik Ü, Suni T, Smolander S, Sogachev A, Launiainen S and Ojala A 2006 Eddy covariance measurements of carbon exchange and latent and sensible heat fluxes over a boreal lake for a full open-water period *J. Geophys. Res.* **111** D11101
- Walter J A, Fleck R, Kastens J H, Pace M L and Wilkinson G M 2021 Temporal coherence between lake and landscape primary productivity *Ecosystems* **24** 502–15
- Wang W, Yi Y, Zhong J, Kumar A and Li S-L 2020 Carbon biogeochemical processes in a subtropical karst river–reservoir system *J. Hydrol.* **591** 125590
- Wanninkhof R, Asher W E, Ho D T, Sweeney C and McGillis W R 2009 Advances in quantifying air-sea gas exchange and environmental forcing *Annu. Rev. Mar. Sci.* **1** 213–44
- Weyhenmeyer G A, Kosten S, Wallin M B, Tranvik L J, Jeppesen E and Roland F 2015 Significant fraction of CO<sub>2</sub> emissions from boreal lakes derived from hydrologic inorganic carbon inputs *Nat. Geosci.* **8** 933–6
- Zhong J, Si-Liang L, Ding H, Lang Y, Maberly S C and Xu S 2018 Mechanisms controlling dissolved CO<sub>2</sub> over-saturation in the three gorges reservoir area *Inland Waters* **8** 148–56
- Zwart J A, Hanson Z J, Read J S, Fienen M N, Hamlet A F, Bolster D and Jones S E 2019 Cross-scale interactions dictate regional lake carbon flux and productivity response to future climate *Geophys. Res. Lett.* **46** 8840–51
- Zwart J A, Hanson Z J, Vanderwall J, Bolster D, Hamlet A and Jones S E 2018 Spatially explicit, regional-scale simulation of lake carbon fluxes *Glob. Biogeochem. Cycles* **32** 1276–93